AIAA Journal

VOLUME 9 APRIL 1971 NUMBER 4

Dynamics of an Explosive Reaction Center

L. J. ZAJAC*
Rocketdyne/North American Rockwell, Conago Park, Calif.

AND

A. K. OPPENHEIM†
University of California, Berkeley, Calif.

The paper presents the first study of the gasdynamic effects of a reaction center in an explosive gas mixture. Initially the center is formed by a certain amount of gas that starts to react within a small region situated in an essentially unconfined space filled with the unreacted gas that remains at a frozen composition. A hydrogen-oxygen system is considered as the reacting medium and a complete set of data on the kinetics of its chain reactions are used to evaluate the resulting chemical and gasdynamic processes. This is obtained by the solution of the set of kinetic rate equations for the chemical system, subject to thermodynamic restrictions imposed by the nonsteady gasdynamic processes of the flowfield generated by the expanding reaction center. The existence of plane, line, or point symmetrical motion is assumed and the analysis is carried out by numerical computations using the method of characteristics for the treatment of the unreacted flowfield. The solution yields information on the gasdynamic phenomena associated with the generation of flow, as well as on the variation of the composition and the energy deposited in the reacting gas with time, demonstrating specifically the influence of geometrical constraints on the coupling between the gasdynamic and kinetic processes that govern the combustion reaction, as manifested especially by the specific power pulse of energy released by the reaction center, and the pressure pulse it generates.

Nomenclature

a = velocity of sound
A = pre-exponential for rate constant
$\mathfrak{a}$ = symbol for chemical species
c = concentration
D = diffusion coefficient
E = activation energy
$\hbar$ = molar enthalpy
h = enthalpy
j = 0,1,2 for plane, cylindrical or spherical flow, respectively
k = rate constant
M = Mach number
$\mathfrak{M}$ = molecular weight
p = pressure
q = specific energy
r = radius
$\mathfrak{R}$ = universal gas constant
s = entropy
t = time
T = temperature
u = particle velocity
V = wave velocity
x = mole fraction
$\Gamma \equiv (\partial \ln p/\partial \ln \rho)_s$
ρ = density
ν = stoichiometric coefficient
ω = specific power

Subscripts

b = backward reaction
f = forward reaction
i = interface or chemical species
k = kernel
0 = initial state
s = surroundings
x = state ahead of shock
y = state behind shock

Received October 15, 1969, presented as Paper 70-147 at the AIAA 8th Aerospace Sciences Meeting, New York, January 19–21, 1970; revision received September 21, 1970. This work was supported by the U.S. Air Force through the Air Force Office of Scientific Research under Grant AFOSR 129-67, by NASA under Grant NsG-702/05-003-050 and by the National Science Foundation under Grant NSF GK-2156. The authors wish to express their appreciation to S. Frolich and K. Tomlinson for their valuable help in the production of the manuscript and to A. Kuhl and D. Kwak for their expert assistance in the computations and the preparation of the graphs.

* Research Engineer. Associate Fellow AIAA.
† Professor. Fellow AIAA.

Background

THE gasdynamic features of explosions associated with combustion processes are, it seems, self-evident. And yet, the analysis of their intimate relationship with chemical reactions escaped the attention of the scientific world for a surprisingly long time.[1]

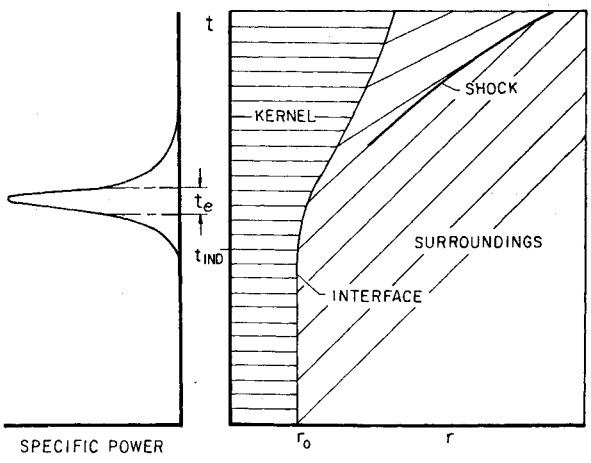

Fig. 1 Schematic diagram of the system.

The fluid-dynamic effects of explosions fascinated the gasdynamicists almost from the advent of this branch of science, as manifested by the early work of Sauer,[2] Schultz-Grunow,[3] and Doering and Burkhardt,[4] and reflected in the classical text of Oswatitsch.[5] However, in these early treatments the combustion process was represented only by the flame front that was considered to act solely as a contact discontinuity devoid of any chemical kinetic properties. In the meantime the interest in the explosion phenomena per se has been greatly enhanced, especially in connection with atomic bombs, which provided a powerful incentive for the development of blast wave theory, leading to the acquisition of an impressive body of knowledge founded upon the classical contributions of Taylor,[6] and Sedov,[7] and followed by Korobeinikov, Mel'nikova and Ryazanov,[8] Sakurai,[9] and many others. So far, however, the blast wave theory has been concerned primarily with the nonsteady flowfield that is obtained as a result of an explosion, rather than with the generation of flow as an integral part of the explosion process and its exothermic reaction.

On the other hand, there have been very few cases where the detailed kinetics of chain reactions of the combustion process have been considered in a gasdynamic flowfield, that is in a flow system of variable density and, of course, pressure, subject to restrictions imposed by the fluid-dynamic boundary conditions. In fact, the only studies known to the present authors have been concerned solely with the essentially steady flowfield of a deflagration in a "laminar" hydrogen-oxygen detonation wave, or, more specifically, with the solution of the kinetic rate equations for the hydrogen-oxygen system, subject to restrictions imposed by the condition of constant mass rate and stream force per unit area known as the Rayleigh line, as exemplified by the early work of Duff,[10] and the more recent investigations of Strehlow and Rubins.[11]

In contrast to such a steady-state flow through a regime of an exothermic reaction, represented on the pressure-specific volume plane by a Rayleigh Line of an essentially negative slope, the salient features of the nonsteady growth of the explosion wave is the fact that in its kernel both the pressure as well as the specific volume increase. This imposes an interesting set of conditions on the chemical system in the course of reaction that, as far as we know, has not been studied before. The major difficulty in such a study is the fact that the progress of the reaction is coupled with the nonsteady gasdynamic phenomena and, unlike other cases, the thermodynamic changes of state cannot be postulated a priori, but, on the contrary, they form one of the features of the solution.

The study reported here represents the initial step in an attempt to fill this gap in our knowledge of explosion processes. More specifically, it addresses itself to the following questions:

1) What is the profile of the *maximum* specific power pulse of energy that can be released and deposited in a given explosive gas as, for instance, in a stoichiometric hydrogen-oxygen mixture, depending on the initial pressure and temperature and the geometrical constraints of the flowfield?

2) What is the profile of the corresponding pressure pulse that arises as a consequence of the gasdynamic flowfield generated in conjunction with the evolution of the power pulse?

To the best of our knowledge these questions have, as yet, remained essentially unexplored although, as already mentioned here earlier, the available data on kinetics, especially for the hydrogen-oxygen system, have been considered sufficiently reliable to investigate on their basis the structure of steady flow, plane, detonation waves.

System

In order to evaluate the maximum specific power pulse, one must consider a system where, on one hand, the energy is deposited in bulk to the whole mass of the medium in the reaction center (rather than just to its portion, diminishing thereby the total) and, on the other, the dissipative effects due to transport phenomena are negligible. The aforementioned two conditions provide criteria for the size of the reaction center, establishing, respectively, the upper and lower bounds of the regime of its physical significance. Both are functions of the duration of the reaction process expressed in terms of the Full Width at Half Maximum (FWHM) of the power pulse.

Considering the high probability of the formation of a localized reaction center (in contrast to a homogeneous reaction process that would involve an extremely accurate simultaneity in the progress of the induction process throughout the medium), the question whether it can undergo the reaction process, once it is formed, without a significant interaction with the surroundings to obliterate the physical significance of its identity, depends on its size which, in turn, is related to the time width of the power pulse. The latter, however, is one of the major unknowns of our problem. Thus one has to have the solution available first, before the physical validity of the model adopted for its derivation can be examined. This is, therefore, carried out here in the Appendix on the basis of the results presented in the main body of the paper, and the consequences of this inquiry are discussed in Conclusions.

The transient flowfield under study is considered to consist of two regions: an expanding kernel, where the chemical reaction takes place while the thermodynamic processes associated with it occur in bulk, and the nonreacting surroundings which are penetrated by a pressure wave that is caused by the expansion of the kernel. The ensuing process is, in effect, that of a closed-loop system, the feedback being associated with the action of the pressure wave generated by the reaction, providing, in turn, for the medium in the kernel the mechanical workload which controls the thermodynamic and chemical processes it undergoes.

The proposed model represents, in effect, the opposite case of a combustion system than that of a flame where the reaction occurs only at the front which moves at a finite velocity with respect to the medium immediately ahead of it. In contrast to this, the reaction center represents a zone of finite volume where the reaction takes place in bulk while its front is a contact discontinuity, that is, its relative velocity with respect to the medium ahead of it is zero.

In this initial study of such a system, the surroundings are assumed to be nonreactive. In an actual explosive medium such a situation cannot, of course, exist indefinitely, since an explosive reaction center leads eventually to the occurrence of other reaction centers around it. Of central importance to this paper is, however, the argument that in an explosive medium the possibility that new centers are formed within the

effective time of the power pulse of a single center is negligible. The quantitative aspects of this argument are presented in the Conclusions. Thus, in effect, the system analyzed here represents the behavior of an essential element of explosion rather than the whole of the explosion process. The latter can be analyzed by considering it, in turn, as a system that is composed of such elementary explosion centers.

The salient features of the system to be thus analyzed are presented in Fig. 1. As implied there, only one-dimensional flow is considered, but, within this restriction, the cases of spherical and cylindrical, as well as plane-symmetrical field are included. The flow system of Fig. 1 represents, in effect, another case of a "bulk expansion" model which has been previously used by us with success for the analysis of the generation of pressure waves in systems undergoing chemical[12,13] as well as nuclear[14-17] reactions. Our former studies were restricted, however, to plane flowfields and they were not related to the kinetics of chemical reactions which, besides the consideration of nonplanar flowfields, forms the primary purpose of the current work.

Analysis

The major simplifying assumption adopted for the present analysis is the postulate that the interface between the kernel and its surroundings is impermeable. As a consequence of this, the interface acts as a contact discontinuity between two regions whose governing equations are thus decoupled from each other. These are then presented here in turn.

Kernel

Since the mass of the kernel is invariant, its density is directly related to the geometric space coordinate in the form of the fcllowing continuity equation:

$$d\rho_k/dt = -\rho_{ko}(d/dt)(r_{io}/r_i)^{j+1} \tag{1}$$

where

$$j \begin{cases} = 0 \text{ for plane symmetrical flowfield} \\ = 1 \text{ for line symmetrical flowfield} \\ = 2 \text{ for point symmetrical flowfield} \end{cases}$$

The equation of state is more conveniently expressed in terms of the perfect gas relation

$$p = c\mathcal{R}T \tag{2}$$

wnere $c = \rho/\mathfrak{M}$ represents the total concentration which is variable in the course of the process so that the substance as a whole is not assumed to behave as a perfect gas.

The variation of concentration is governed by the kinetic rate equations for each of the r elementary steps in the chain sequence involving m species $\mathfrak{A}_i$

$$\sum_{i=1}^{m} \nu_{i,r}' \mathfrak{A}_i \underset{k_{b,r}}{\overset{k_{f,r}}{\rightleftharpoons}} \sum_{i=1}^{m} \nu_{i,r}'' \mathfrak{A}_i \qquad r = 1, \ldots s \tag{3}$$

where

$$k = AT^n \exp(-E/\mathcal{R}T) \tag{4}$$

are the reaction rate constants. From these, for a given constituent $\mathfrak{A}_i$, one obtains

$$\left(\frac{\partial c_i}{\partial t}\right)_\rho = \sum_{r=1}^{s} (\nu_{i,r}'' - \nu_{i,r}') \left[k_{f,r} \prod_{i=1}^{m} c_i^{\nu_{i,r}'} - k_{b,r} \prod_{i=1}^{m} c_i^{\nu_{i,r}''} \right] \tag{5}$$

Since $c_i = x_i c = x_i \rho/\mathfrak{M}$, it follows that

$$(\partial c_i/\partial \rho)_t = (\partial/\partial \rho)(x_i \rho/\mathfrak{M}) = x_i/\mathfrak{M} \tag{6}$$

and, consequently,

$$dc_i/dt = (\partial c_i/\partial t)_\rho + (x_i/\mathfrak{M}) d\rho/dt \tag{7}$$

whence the total concentration is determined as, of course,

$$c = \sum_{i=1}^{m} c_i$$

Finally, the total energy equation is given by

$$dh/dp = 1/\rho \tag{8}$$

where

$$h = \sum_{i=1}^{m} \frac{c_i \tilde{h}_i}{\rho}$$

while

$$\tilde{h}_i = \mathcal{R}T \left[\sum_{n=0}^{5} \frac{a_{ni}(T.10^{-3})^n}{n+1} + \frac{a_{6i}}{T} \right]$$

is evaluated from the JANAF Tables[18] by means of a fifth degree polynomial fit.

Surroundings

The flowfield in the surroundings is evaluated by the method of characteristics with proper account taken of shock fronts when they are formed within the compression wave generated by the expanding kernel. Until that time the flowfield is homogeneously isentropic, that is, the entropy is not only conserved along the particle paths, but also along the characteristics for which, taking proper account of the thermodynamic properties of the substance,[24]

$$du = \mp a[(1/\Gamma) d \ln p + (ju/r)dt] \tag{9}$$

where

$$\Gamma \equiv (\partial \ln p/\partial \ln \rho)_s = (\rho/p)a^2 \tag{10}$$

Since the surrounding medium is considered to remain at "frozen" composition, it behaves, in effect, as a perfect gas, and consequently $\Gamma = \Gamma(T)$. Moreover, since the temperature variation in the surroundings is relatively small, we have assumed for each case that $\Gamma = \Gamma_0 = \text{const}$, introducing thereby a negligible error in the results, while simplifying considerably the computational procedure. However, in order to take properly into account the thermodynamic properties of the substance, the value of Γ_0 has been carefully determined for each initial temperature using the technique of Ref. 24.

Interface

Since the interface is assumed to be impermeable, matching conditions at the contact discontinuity consist of the requirement of pressure balance at its surface:

$$p_{ki} = p_{si} \tag{11}$$

and of the statement that it acts as a piston, that is

$$dr_i/dt = u_i \tag{12}$$

whence by virtue of Eq. (1),

$$d\rho_k/dt = (j+1)(\rho_{ko}/r_i)(r_{io}/r_i)^{j+1} u_i \tag{13}$$

Computations

A code in FORTRAN for the CDC 6400 digital computer was developed to obtain numerical solutions. The code can accommodate any number of elementary kinetic steps describing the chemical reaction in the kernel. The present work uses the kinetic scheme proposed by Skinner and Ringrose[20] for the hydrogen-oxygen system. This scheme consists of 22 forward and backward elementary steps of the type of

Table 1 Kinetic scheme for the hydrogen-oxygen system and the parameters of the reaction rate constants $k = AT^n \exp(-E/RT)$ where k is in (cm³/mole)/sec or (cm³/mole)²/sec, T in °K, and E in kcal/mole

	Reaction	Forward			Backward		
		A	n	E	A	n	E
1	$H_2 + O_2 \leftrightharpoons 2OH$	2.50×10^{14}	0	67	7.05×10^{12}	0	48.60
2	$H + O_2 \leftrightharpoons OH + O$	1.00×10^{15}	0	17.75	6.16×10^{13}	0	1.19
3	$O + H_2 \leftrightharpoons OH + H$	1.20×10^{13}	0	9.20	5.50×10^{12}	0	7.37
4	$OH + H_2 \leftrightharpoons H_2O + H$	1.48×10^{14}	0	6.43	6.92×10^{14}	0	21.62
5	$OH + OH \leftrightharpoons H_2O + O$	7.40×10^{14}	0	3.82	7.60×10^{15}	0	20.84
6	$H + O_2 + M \leftrightharpoons HO_2 + M$	8.25×10^{15}	0	0	1.01×10^{20}	−1	50
7	$HO_2 + H_2 \leftrightharpoons H_2O_2 + H$	3.20×10^{16}	0	34.60	2.46×10^{16}	0	18.22
8	$H + H + M \leftrightharpoons H_2 + M$	1.50×10^{18}	−1	0	3.48×10^{22}	−2	108
9	$H + OH + M \leftrightharpoons H_2O + M$	3.60×10^{19}	−1	0	3.95×10^{24}	−2	123.20
10	$H + H + H_2O \leftrightharpoons H_2 + H_2O$	3.00×10^{19}	−1	0	6.96×10^{23}	−2	108
11	$H + OH + H_2O \leftrightharpoons H_2O + H_2O$	7.20×10^{20}	−1	0	7.90×10^{25}	−2	123.20

Eq. (3). The parameters of their rate constants, as defined by Eq. (4), are given in Table 1.

In all, eight species are considered as constituents, namely H_2, O_2, H_2O, H, OH, O, HO_2, and H_2O_2. The kinetic scheme is expressed therefore by eight simultaneous, nonlinear differential equations of the type of Eq. (5). The total time variation of the constituents in the kernel is determined from Eqs. (7) which are integrated by means of a fourth-order Runge-Kutta technique. The routine features a self-readjusting integration step size, introduced by Hirsch and Ryason[21] to maintain a small error in the dependent variables. Unlike other methods of numerical integration, the Runge-Kutta method does not permit a mathematically rigorous error treatment. A usual "rule of thumb" approximation is obtained for this purpose by assuming that the error incurred in a given step is proportional to the step size raised to the fifth power.

Thus, with reference to Fig. 2, the step size, Δt_k, is readjusted after each three integration steps in the following manner: the integration is repeated over the time interval t_1 to t_3 using a single step size of $2\Delta t_k$. New values of the dependent variables, $c_{i,3'}$ ($i = 1, \ldots 8$) are obtained at time t_3. In order to double the step size, the condition

$$|c_{i,3'} - c_{i,3}|/(2^5 - 2)c_{i,1} < 10^{-8} \tag{14}$$

is imposed on all the values of i for which $|c_{i,1}|$ exceeds 10^{-25} moles/liter. If this condition is not met, a new step size Δt_k^*, which satisfies this requirement is determined on the basis of Eq. (14), namely:

$$\Delta t_k^* = [\{(2^5 - 2)c_{i,1}/|c_{i,3'} - c_{i,3}|\}\ 10^{-8}]^{1/5}\Delta t_k \tag{15}$$

As pointed out in the previous section, the flowfield in the surroundings is evaluated numerically by the method of characteristics with $\Gamma_0 = \Gamma(T)$ evaluated on the basis of the JANAF Tables[18] and listed in Table 2. The finite difference network used for this purpose is a slightly modified version of the standard approach[19,22] and it is presented by Fig. 3. The

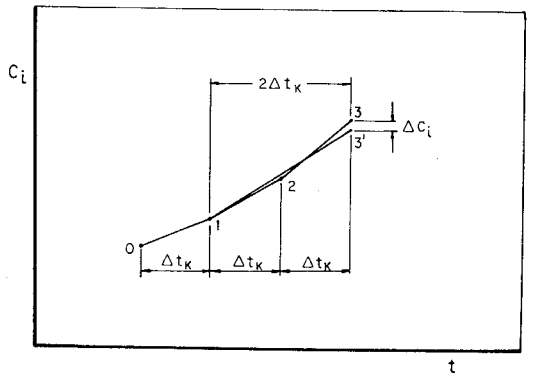

Fig. 2 Schematic diagram of the integration routine.

advantage of this network is that it yields a complete solution in the surroundings for a single time step while maintaining the continuity of the C_+ characteristics for the detection of shock formation. In addition, since network points are added at the interface, it retains the desirable feature of having the greatest point density in the region of largest gradients.

The flow in the surroundings is characterized by a relatively small inactive gasdynamic period, corresponding to the induction time of the reactive gas, followed by a rapid compression caused by the exploding kernel. To reduce the computation time, the reaction in the kernel is considered to occur at constant volume until the pressure increases by an amount equal to 0.01% of its initial value. The pressure in the surroundings is then adjusted to this value and the kernel allowed to expand. When compared to the solution where a continuous expansion of the kernel throughout the induction period was taken into account, this technique was found to yield sufficiently accurate results.

The time step in the surroundings is determined from the requirement that the C_- characteristic intersect the constant time line near a given network point, Fig. 3. Hence,

$$\Delta t_s = \Delta\bar{r}/2\bar{a} \tag{16}$$

where $\Delta\bar{r}$ is the average distance between network points and $\bar{a}$ is the average velocity of sound.

For nonplanar geometry, the step size is restricted by the initial radius of the kernel. This is due to the conditions imposed by Eq. (9) that, in difference form, require the second term on the right side to be sufficiently small in order to assure convergence. Hence, for this purpose, one has to have

$$\Delta t_s \ll 2r_i/ja_i \tag{17}$$

Choosing a general criterion

$$\Delta t_s = 0.1r_i/(j + 1)a_i \tag{18}$$

has, from our experience, been quite adequate for all the geometrical conditions of the flowfield.

During the explosive portion of the process, it is advantageous to have a time step that is sensitive to the rate of expansion of the kernel. For this purpose a second criterion for the time step is chosen as

$$\Delta t_s = 0.01p_i|dp_i/dt|^{-1} \tag{19}$$

Table 2 Values of $\Gamma \equiv (\partial \ln p/\partial \ln \rho)_s$ determined on the basis of JANAF Tables[18] for a stoichiometric hydrogen-oxygen mixture and used for the computations reported in this paper

T (°K)	900	1100	1200	1400
Γ	1.360	1.349	1.344	1.333

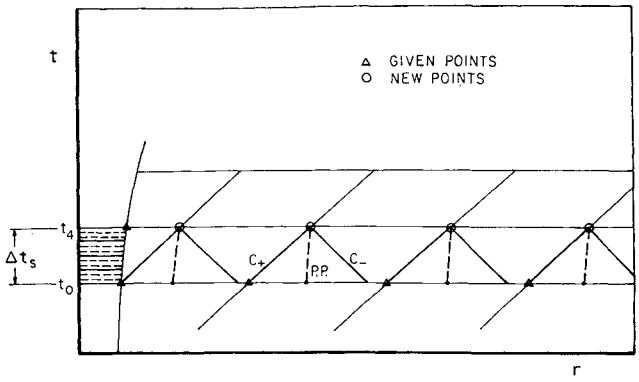

Fig. 3 Schematic diagram of the characteristic network.

where, as before, in our experience the coefficient has been found to yield satisfactory results. The time step in the surroundings at any time is then the smallest value computed from either Eq. (18) or Eq. (19). In accordance with Eq. (16) points are added to the characteristic network at every other time step.

For convenience, the time step used for matching the boundary conditions at the interface was taken to be

$$\Delta t_i \leq 3\Delta t_k \tag{20}$$

the equal sign holding when $\Delta t_s \geq 3\Delta t_k$.

The computations are performed in three stages: 1) integration of the kinetic rate equations in the kernel for an assumed value of $d\rho/dt$, 2) matching of the boundary conditions at the interface yielding a corrected value of $d\rho/dt$, and 3) when stages 1 and 2 have converged, the solution of the flowfield in the surroundings. A detailed description of the numerical technique is presented in the Appendix.

Results

As an illustration of the results we have obtained in this manner, presented here are data corresponding to a stoichiometric hydrogen-oxygen mixture initially at 1100°K and 6 atm, with an initial kernel radius of 0.1 mm. The nonsteady flow field generated by the explosion process is depicted on Fig. 4, showing the trajectories of the interfaces and shock waves, as well as a few representative characteristics for the three geometric cases of plane, cylindrical and spherical gas motion. Shock waves were generated only in the case of plane and cylindrical fields, the increase of the cross-sectional area in the spherical case having been evidently too large for this purpose.

The influence of the geometry is perhaps even more prominently displayed by the pressure pulses shown on Fig. 5 and by the corresponding variation of the interface velocity given

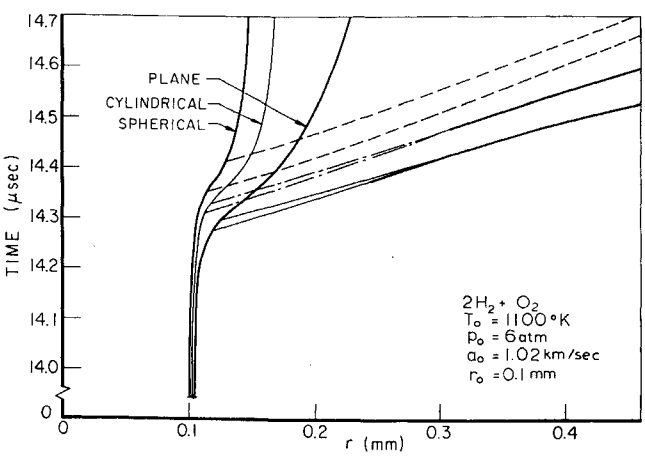

Fig. 4 The time-distance diagram of the process.

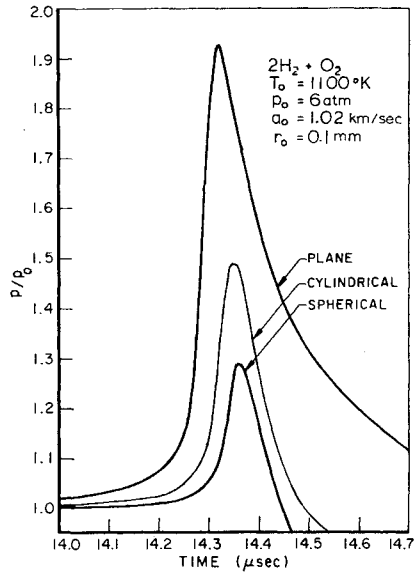

Fig. 5 Time profiles of the pressure in the kernel.

by Fig. 6. The latter is, in effect, the time derivative of the specific volume whose variation, together with the pressure pulse data of Fig. 5, provides the required information for the representation of the explosion process on the pressure-specific volume plane, represented on Fig. 7. As it appears there, initially there is an increase in both pressure and specific volume so that the process path starts with a positive slope, and only later, as the pressure pulse decays, does it become negative, similarly as in a steady flow process.

The temperature variation in the kernel is depicted on Fig. 8 together with the time profile of the effective heat of formation

$$q = (1/\mathfrak{M}_0)\Sigma x_{io}\mathfrak{H}_{io} - (1/\mathfrak{M})\Sigma x_i\mathfrak{H}_{i@T_0} \tag{21}$$

where, in terms of the nomenclature of the JANAF Tables[18]

$$\mathfrak{H} \equiv H^0 - H_{298}{}^0 + \Delta H_f{}^0$$

while x_i is the mole fraction of a constituent at any given state and, $\mathfrak{M}$ is the molecular weight of the mixture.

The effective heat of formation q represents the specific energy deposited in the medium as a consequence of the exo-

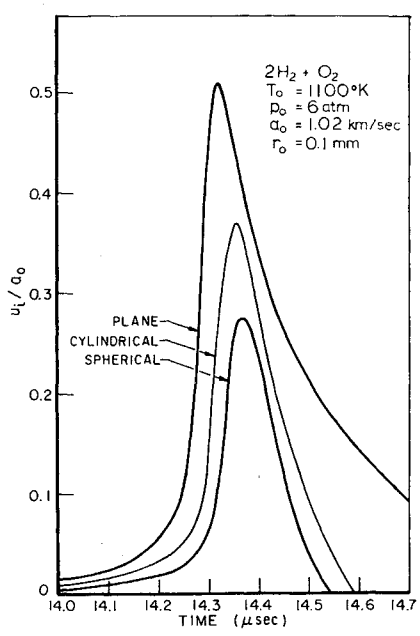

Fig. 6 Time profiles of the kernel front velocity.

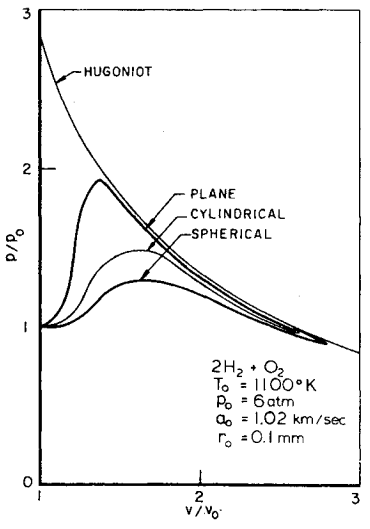

Fig. 7 The pressure-specific volume diagram of the process in the kernel.

thermic process. Its rate of change expresses then the specific power of the explosion process, ω. The time profile of the latter, obtained by straightforward differentiation of q with respect to time, is presented on Fig. 9. The graph reveals the fact that the variation of ω is associated with two peaks—a feature especially well pronounced in the case of plane geometry. This is a direct result of the fact that the exothermic reactions achieve maximum rates when the concentration products $[H]^2$ or [H][OH], corresponding to the recombinations of hydrogen atoms and hydrogen-hydroxyl radicals, respectively, that are associated with the highest reaction heats, are at their maximum. This is demonstrated by the plots of the mole fractions of H and OH shown in the upper diagram of Fig. 9.

Conclusions

Figures 4–9 represent sample solutions of our problem. Specifically, for example, the answer to the questions posed at the outset appears from them to be as follows: in a stoichiometric hydrogen-oxygen mixture, at an initial temperature of 1100°K and initial pressure of 6 atm, a spherical reaction center of an initial radius of 100 μ can, at most, deposit energy at a rate corresponding to a specific power pulse of 74 nsec (FWHM) with a peak at 76 Gw/g, generating a pressure pulse of 76 nsec (FWHM) reaching a peak of 7.7 atm.

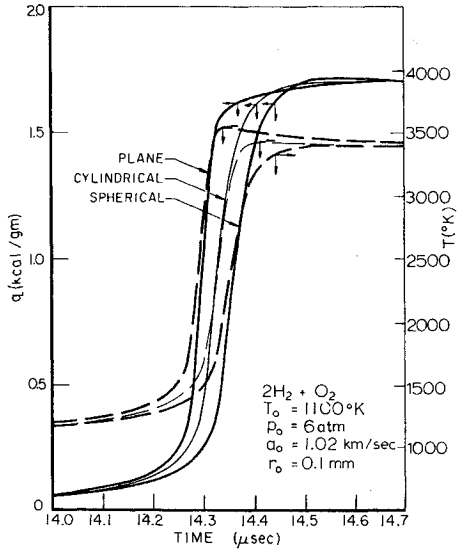

Fig. 8 Time profiles of the temperature and energy conversion in the kernel.

Corresponding values for other flow geometries are of the same order of magnitude and they can be read off the graphs, given by Figs. 4–9.

Similar computations were carried out for $r_0 = 0.1$ mm. over a range of initial pressures at a constant initial temperature of 1100°K and for $r_0 = 1$ mm over a range of initial temperatures at a constant initial pressure of 1 atm. The results, all for spherical geometry, are shown on Fig. 10. As it is evident there, both the magnitude and sharpness of the pulses of specific power and pressure depend greatly on initial pressure, while remaining relatively little influenced by the variation in initial temperature.

Finally, it should be noted that, although our results give the *maximum* values for these pulses, which, as demonstrated in the Appendix, can be, indeed, expected to occur in a physical system, they represent at the same time a conservative estimate of the eventual outcome of the explosion process in a reacting medium. The reason for this is the fact that the flow-field generated by a reaction center enhances the termination of the induction process in the surrounding medium and thus it can lead to the generation of other reaction centers in its neighborhood. However one should also observe that the period of an order of 100 nsec which, as shown here, represents the FWHM duration of the power pulse is extremely short in comparison to the tens of microseconds taken up by the induction process at the same initial conditions. Thus, since the corresponding nonsimultaneity of 1% is certainly quite reasonable to expect for the onset of reaction in various centers within an explosive gas mixture, one is led to the conclusion that such reaction centers are in time chemically isolated from each other. Moreover, since, as shown on Fig. 9, the concentration of the hydrogen atom, the most important active species, varies in form of a pulse whose FWHM is of the same order of magnitude as that of the power pulse, it follows that, if initially there has been a somewhat delayed build-up in the concentration of this radical in the immediate neighborhood of the reaction center, in the second half of the power pulse this will be depleted as a consequence of the negative gradient associated with its consumption in the reaction center.

This means that, in contrast to the close coupling between the chemical kinetic and gasdynamic processes that, as shown here, must exist in any reaction center, the processes in various reaction centers that are distributed throughout the

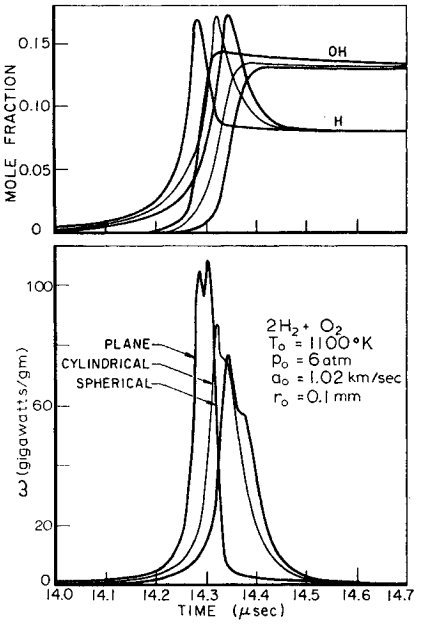

Fig. 9 Time profiles of the specific power of energy conversion and the mole fractions of H and OH in the kernel.

explosive gas mixture are chemically decoupled. It is this notion, in fact, that makes the results of our analysis especially significant, because they can be consequently regarded as describing the behavior of an elementary reaction center whose chemical behavior is not influenced by the action of other reaction centers in its neighborhood.

Appendix: Technique of Numerical Analysis

Introducing, to represent the mean value of any quantity f, the symbol $\langle f\rangle_n{}^m$, defined as

$$\langle f\rangle_n{}^m \equiv \tfrac{1}{2}(f_m + f_n) \tag{A1}$$

the energy equation for the kernel, Eq. (8), can be expressed in finite difference as

$$(h_m - h_n)\langle\rho\rangle_n{}^m = (p_m - p_n) \tag{A2}$$

Similarly, the characteristics equations for the flow in the surroundings, Eqs. (15), become, with the use of Eq. (17),

$$u_m - u_l = -(1/\Gamma)\langle a/p\rangle_l{}^m(p_m - p_l) - j\langle au/r\rangle_l{}^m\Delta t_s \tag{A3a}$$

and

$$u_m - u_n = (1/\Gamma)\langle a/p\rangle_n{}^m(p_m - p_n) + j\langle au/r\rangle_n{}^m\Delta t_s \tag{A3b}$$

while Eqs. (14) are represented simply as

$$(r_m - r_l) = \langle u + a\rangle_l{}^m\Delta t_s \tag{A4a}$$

and

$$(r_m - r_n) = \langle u - a\rangle_n{}^m\Delta t_s \tag{A4b}$$

The trajectory of a particle or shock is, on the basis of Eqs. (16) and (21), given, respectively, by

$$(r_m - r_n) = \langle u\rangle_n{}^m\Delta t_s \tag{A5}$$

and

$$(r_m - r_p) = \langle V\rangle_p{}^m\Delta t_s \tag{A6}$$

In the following, the flow properties at points lying between given network points are determined by linear interpolation.

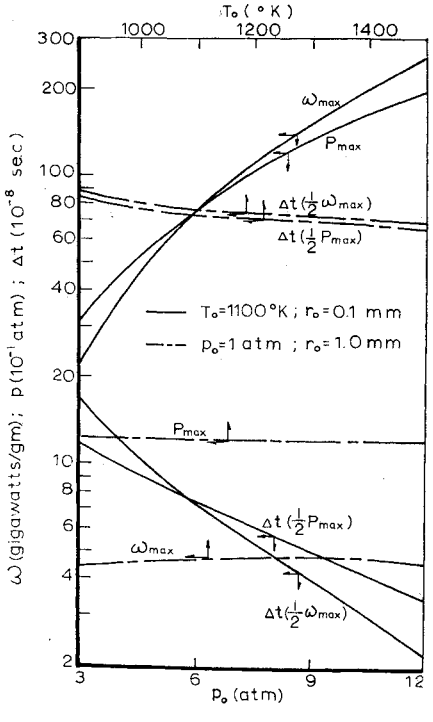

Fig. 10 Salient features of the specific power and pressure pulses.

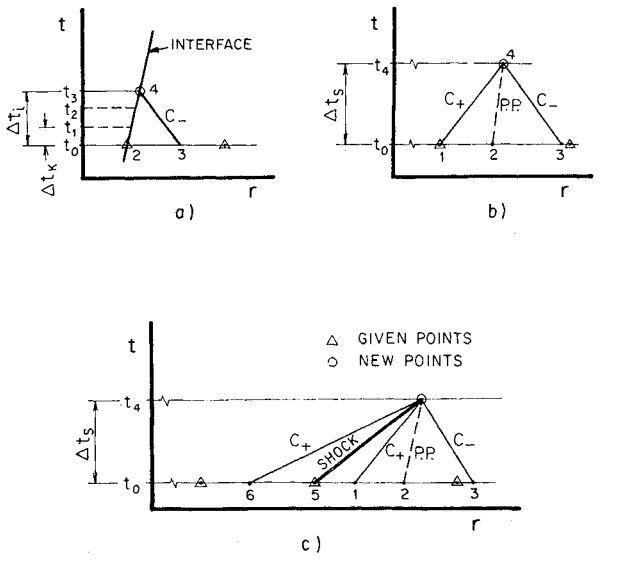

Fig. 11 Finite-difference networks used in the numerical analysis.

Kernel

Given the solution at time t_0, Fig. 11a, a choice is made for $\langle d\rho/dt\rangle_{t_0}{}^{t_3}$. The density, ρ_{t_1}, is then computed from

$$\rho_{t_1} = \rho_{t_0} + \langle d\rho/dt\rangle_{t_0}{}^{t_3}\Delta t_k \tag{A7}$$

and the concentrations at time t_1 are obtained by numerical integration of Eqs. (7) where $d\rho/dt$ is replaced by its average value over the interval t_0 to t_3. Next, the energy equation, Eq. (A2), being a function of temperature only [the pressure having been eliminated by the use of the equation of state, Eq. (2)], is solved for T_{t_1}, by the method of "Regula Falsi."[23] The pressure, p_{t_1}, is then determined from Eq. (2).

Maintaining the assumed value for $\langle d\rho/dt\rangle_{t_0}{}^{t_3}$, the above routine is repeated twice more until the time t_3 is reached. The condition of equal pressure across the interface yields a corrected value of $\langle d\rho/dt\rangle_{t_0}{}^{t_3}$.

Interface

Having established the pressure in the kernel at time t_3, the remaining flow variable at the interface may be found. Referring again to Fig. 11a, the velocity of sound at point 4 may be found directly from the isentropic relation

$$a_4 = a_2(p_4/p_2)^\alpha \tag{A8}$$

where

$$\alpha = (\Gamma - 1)/2\Gamma$$

while, by virtue of Eq. (22),

$$p_4 = p_{ki} = p_{t_3} \tag{A9}$$

Assuming u_4, u_3 and a_3, the spatial positions of points 4 and 3 are determined from Eqs. (A5) and (A4b), respectively. The particle velocity u_4 is then obtained from the equation for the C_- characteristic, Eq. (A3b). Finally, the density derivative in the kernel at time t_3, is evaluated from Eq. (24) and an improved value of $\langle d\rho/dt\rangle_{t_0}{}^{t_3}$ computed. The solution in the kernel and at the interface is iterated until $(d\rho/dt)_3$ converges. Generally, two iterations are sufficient.

Surroundings

The solution at a general point in the surroundings is determined from the network depicted on Fig. 11b. Assuming initial values for u_3, u_4, a_3, and a_4, the locations of the new point 4 and point 3 are determined from Eqs. (A4). Equa-

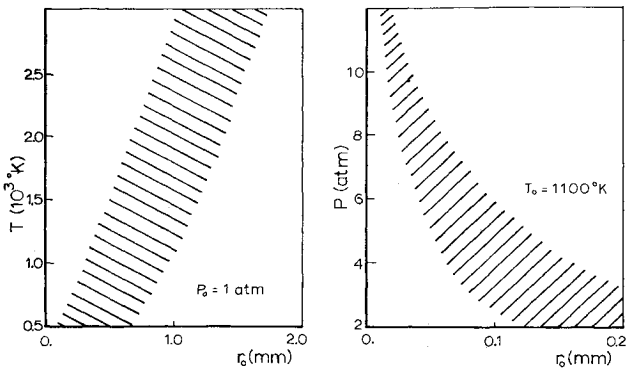

Fig. 12 Regimes of physical validity of the explosive reaction center in a stoichiometric hydrogen-oxygen system.

tions (A3) are then solved simultaneously for the particle velocity, u_4, and pressure, p_4. For homentropic flow, the velocity of sound, a_4, is evaluated by applying Eq. (A3) along the C_+ characteristic. If the flow is not homentropic, the third characteristic direction, Eq. (A5) is used to locate point 2 and the velocity of sound at point 4 is determined from Eq. (A8) applied along the particle path.

An additional routine is required to include shock fronts in the computation. The network used is shown on Fig. 11c for the general case of a shock propagating into a non-uniform region. Assuming that $M_4 = M_5$ while the properties ahead of the shock at point 4 are the same as those ahead of it at point 5, the location of the new point r_4, is obtained from Eq. (A6). Equation (A4a) locates point 6 and Eq. (A3a) is used to determine pressure p_{4y}. A corrected value of M_5 is then obtained from Eq. (18) while u_{4y} and a_{4y} are evaluated from the remaining jump conditions, Eqs. (19) and (20). Improved values of u_{4x}, p_{4x}, and a_{4x} are finally computed in a manner similar to the general point routine described above. The solution is repeated until the properties at point 4 converge.

Shock formation is detected by the coalescence of two C_+ characteristics. When this occurs, the first C_+ characteristic is replaced by a shock with $M = 1$ and the new point computed by the use of the shock routine.

Limit of Physical Validity

The behavior of an explosive reaction center is associated with two conditions: 1) the interface between the kernel and the surroundings is impermeable to transport phenomena, 2) internal properties within the kernel are uniformly distributed throughout its volume. The first condition establishes a criterion for the minimum radius of the kernel, while the second, for its maximum size.

In order for the interface to maintain the property of a discontinuity as an impermeable membrane, the initial jump of potential governing the transport of mass or heat must not be significantly distorted by diffusion during the duration of the power pulse. Expressing this potential in terms of $F \equiv (f - f_s)/(f_k - f_s)$, where f represents the concentration of active species or the temperature, while subscript k and s denote its inital value in the kernel and surroundings respectively, the diffusion equation can be written as

$$\partial F/\partial \tau - (j/\xi)\partial F/\partial \xi - \partial^2 F/\partial \xi^2 = 0 \qquad \text{(A10)}$$

where $\tau \equiv Dt/r_0^2$ represents the nondimensional time and $\xi \equiv r/r_0$, the nondimensional radius. For $j = 2$, the solution of Eq. (A10), subject to initial conditions: $F(\xi,0) = 1$ at all $|\xi| < 1$ and $F(\xi,0) = 0$ at all $|\xi| > 1$, can be expressed as

$$F = \tfrac{1}{2}\,\mathrm{erf}w + \tfrac{1}{2}\,\mathrm{erf}z + \xi^{-1}(\tau/\pi)^{1/2}(e^{-w^2} - e^{-z^2}) \qquad \text{(A11)}$$

where $w \equiv (1 - \xi)/2(\tau)^{1/2}$ and $z \equiv (1 + \xi)/2(\tau)^{1/2}$. From the preceding, it follows that in the center

$$F_{\xi=0} = \mathrm{erf}(\tfrac{1}{2}t^{-1/2}) - (\pi t)^{-1/2}\exp(-1/4\tau) \qquad \text{(A12)}$$

Adopting as a reasonable criterion the postulate that the distortion in the profile of the potential F must not affect its value in the center by more than a factor of 10^{-3}, one obtains from Eq. (A12) the condition

$$\tau < 0.02$$

or

$$r_0 > 7(Dt_e)^{1/2} \qquad \text{(A13)}$$

where $t_e = \Delta t_{(\frac{1}{2}\omega_{max})}$.

In order for the internal properties of the kernel to be uniformly distributed throughout its volume, the gasdynamic processes it undergoes must be closely coupled over its entire regime. Since the interactions that provide such a coupling are propagated through the space at the local velocity of sound, most conservatively this condition yields the criterion.

$$r_o < a_o t_e \qquad \text{(A14)}$$

where a_0 is the initial velocity of sound in the reacting medium—the lowest value it has throughout the whole process.

The regime of physical validity of the reaction center evaluated on the basis of the above criteria is presented on Fig. 12. Used for this purpose were the values of $\Delta t(\frac{1}{2}\omega)$ given by Fig. 10, combined with the most conservative estimate for the diffusion coefficient, namely D_{H-H_2} as quoted as a function of temperature by Fristrom and Westenberg[25] at a pressure of 1 atm and extrapolated to higher pressures by assuming that the diffusion is inversely proportional to pressure. From Fig. 12 it appears that the value of 100 μ used for all the results presented in the paper lies, indeed, with the notable exception of those corresponding to high initial pressures, well within the regime of physical validity.

References

[1] Oppenheim, A. K., "The No-Man's Land of Gasdynamics of Explosions," *Applied Mechanics Review*, Vol. 20, No. 4, April 1967, pp. 313–319.

[2] Sauer, R., "Charakteristikenverfahren fur Kugel-und Zylinderwellen reibungsloser Gase," *Zeitschrift fur angewandte Mathematik und Mechanik*, Vol. 23, No. 1, Feb. 1943, pp. 29–32.

[3] Schultz-Grunow, F., "Zur Behandlung nichtstationarer Verdichtungsstosse und Detonationswellen," *Zeitschrift fur angewandte Mathematik und Mechanik*, Vol. 24, Nos. 5 & 6, June 1944, pp. 284–288.

[4] Doering, W. and Burkhardt, G., "Contributions to the Theory of Detonation," *Förschungsbericht der Deutschen Luftfahrtforschung*, 1939, 1944, Berlin; transl. TR F-TS-1227-IA (GDAM A9-T-46), 1949, Wright-Patterson Air Force Base, Ohio.

[5] Oswatitsch, K., *Gas Dynamics*, transl. by G. Kuerti, Academic Press, New York, 1956, pp. 168–172.

[6] Taylor, G. L., "The Formation of a Blast Wave by a Very Intense Explosion. I. Theoretical Discussion" and "II. The Atomic Explosion of 1945," *Proceedings of the Royal Society*, Vol. A201, March 1950, pp. 159–174, 175–186.

[7] Sedov, L. I., *Similarity and Dimensional Methods in Mechanics*, trans. by M. Friedman, edited by M. Holt, Academic Press, New York, 1959.

[8] Korobeinikov, V. P., Mel'nikova, N. S., and Ryazanov, Y. V., *Teoriya Tochechnovo Vzryva*, Moscow, 1961; transl. "The Theory of Point Explosions," JPRS: 14, 334, July 1962, U.S. Department of Commerce, Washington, D.C.

[9] Sakurai, A., "On the Propagation and Structure of the Blast Wave: I" "I", *Journal of the Physical Society of Japan*, Vol. 8, No. 5, May 1953, pp. 662–669; and "On the Propagation and Structure of the Blast Wave: II," *Journal of the Physical Society of Japan*, Vol. 9, No. 2, Feb. 1954, pp. 256–266.

[10] Duff, R. E., "Calculation of Reaction Profiles Behind Steady-State Shock Waves," *The Journal of Chemical Physics*, Vol. 28, No. 6, June 1958, pp. 1193–1197.

[11] Strehlow, R. A. and Rubins, P. M., "Experimental and Analytical Study of H_2-Air Reaction Kinetics Using a Standing-

Wave Normal Shock," *AIAA Journal*, Vol. 7, No. 7, July 1969, pp. 1335–1344.

[12] Busch, C. W., Laderman, A. J., and Oppenheim, A. K., "Pressure Wave Generation in Particle-Fueled Combustion Systems: I. Parametric Study," *AIAA Journal*, Vol. 4, No. 9, Sept. 1966, pp. 1638–1644.

[13] Busch, C. W. et al., "Pressure Wave Generation in Particle Fueled Combustion Systems: II. Influence of Particle Motion," *AIAA Journal*, Vol. 6, No. 2, Feb. 1968, pp. 286–291.

[14] Smith, H. P., Jr., Busch, C. W., and Oppenheim, A. K., "Pressure Wave Generated in a Fissionable Gas by Neutron Irradiation," *The Physics of Fluids*, Vol. 7, No. 5, May 1964, pp. 676–682.

[15] Smith, Jr., H. P., Evans, R. D., Busch, C. W. and Oppenheim, A. K., "Pressure Wave Generation in a Fissioning Gas: II. Effects of Dissociation and Multiphase Composition," *The Physics of Fluids*, Vol. 8, No. 8, Aug. 1965, pp. 1421–1423.

[16] Busch, C. W., Oppenheim, A. K., and Smith, H. P., Jr., "Pressure Wave Generation in a Fissioning Gas: III. Amplification of the Pressure Pulse with Helium 3 as Driver," *The Physics of Fluids*, Vol. 9, No. 4, April 1966, pp. 813–814.

[17] Podney, W. N., Smith, Jr., H. P., and Oppenheim, A. K., "On the Generation of a Fissioning Plasma in a Shock Tube," *Proceedings of the Sixth International Shock Tube Symposium*, Freiburg, April 1967; also *The Physics of Fluids*, Vol. 12, No. 15, May 1969, pp. I 68–I 72.

[18] Stull, D. R., "JANAF Thermochemical Tables," The Thermal Research Lab., Aug. 1965, Dow Chemical Co., Midland, Mich.

[19] Rudinger, G., *Wave Diagrams for Nonsteady Flow in Ducts*, D. Van Nostrand, New York, 1955.

[20] Skinner, G. B. and Ringrose, G. H., "Ignition Delays of a Hydrogen-Oxygen-Argon Mixture at Relatively Low Temperatures," *Journal of the Chemical Society (London)*, Vol. 42, No. 6, June 1965, pp. 2190–2192.

[21] Hirsch, E. and Ryason, P. R., "A Study of the Hydrogen-Oxygen Reaction," *The Journal of Chemical Physics*, Vol. 40, No. 7, April 1964, pp. 2050–2051.

[22] Shapiro, A. H., *The Dynamics and Thermodynamics of Compressible Fluid Flow*, Vol. II, Chaps. 24 and 25, Ronald Press, New York, 1953.

[23] Korn, G. A. and Korn, T. M., *Mathematical Handbook for Scientists and Engineers*, McGraw-Hill, New York, 1961.

[24] Zajac, L. J. and Oppenheim, A. K., "Thermodynamic Computations for the Gasdynamic Analysis of Explosion Phenomena," *Combustion and Flame*, Vol. 13, No. 5, Oct. 1969, pp. 537–550.

[25] Fristrom, R. M. and Westenberg, A. A., *Flame Structure*, McGraw-Hill, New York, 1965, p. 281.

APRIL 1971 AIAA JOURNAL VOL. 9, NO. 4

Coupled Nongray Radiating Flows about Long Blunt Bodies

LINWOOD B. CALLIS*
NASA Langley Research Center, Hampton, Va.

Second-order time asymptotic solutions extending far downstream are presented for hypervelocity blunt-body flowfields including coupled nongray radiation. Shapes considered are sphere-cones and blunted conical shapes with continuous curvature. Numerical calculations treat the shock as a discrete surface, and it is assumed that the flow is inviscid, nonconducting, and axisymmetric. Thermochemical equilibrium is assumed. Radiation is accounted for with an eight-step model absorption coefficient including line, band, and continuum radiation. Results include shock shapes, radiative heating distributions, and profiles through the shock layer of pertinent thermodynamic and flow quantities. A parametric analysis is made of radiating flows over sphere-cones. Comparisons with other investigators are made, where possible.

Nomenclature

A,B,C,D,E = defined by Eq. (5)
B_ν = nondimensional blackbody function
$\bar{c}$ = speed of light, m/sec
E_n = exponential integral function of order n, $E_n(y) = \int_1^\infty e^{-yt}\, t^{-n}\, dt$
F^R = nondimensional divergence of the radiation flux vector
g = general parameter representing ρ,u,v, or p
h = nondimensional enthalpy
$\bar{h}_P$ = Planck's constant, joule-sec
I_ν = nondimensional specific radiation intensity
K = defined by Eqs. (5)
$\bar{k}$ = Boltzmann constant, joules/°K
P_1,P_3 = defined by Eqs. (5)
p = nondimensional pressure
q^R = nondimensional radiative heat flux to body
$\bar{R}_N$ = nose radius, m
r = nondimensional radial coordinate
s = nondimensional radiation path length
T = nondimensional temperature where indicated
T,t',t = nondimensional time
u,v = nondimensional velocity components, body-oriented system
$\bar{V}_\infty$ = freestream velocity, m/sec
x,y = nondimensional body-oriented coordinates
x',y' = nondimensional Cartesian coordinates
X,Y = nondimensional floating coordinates
$\bar{Z}$ = altitude, km
β = local shock angle relative to body, radians
δ = nondimensional standoff distance
ϵ = defined by Eqs. (5)
θ = body surface inclination, rad
λ = defined by Eqs. (5)
ν = nondimensional radiation frequency
ρ = nondimensional density
ρk = nondimensional absorption coefficient
ρk_P = nondimensional Planck mean absorption coefficient
$\bar{\sigma}$ = Stefan-Boltzmann constant, $w/(m^2 - °K^4)$
τ = optical thickness
ω = solid angle

Subscripts

c = asymptotic or conical angle
o = standard conditions
st = stagnation conditions

Presented as Paper 70-865 at the AIAA 5th Thermophysics Conference, Los Angeles, Calif., June 29–July 1, 1970; submitted July 31, 1970; revision received October 22, 1970.

* Aero-Space Technologist, Gas Radiation Section, Hypersonic Vehicles Division.